5.2 SEASONAL TRANSITIONS OF ZONALLY SYMMETRIC CIRCULATIONS

William R. Boos*
Massachusetts Institute of Technology, Cambridge, Massachusetts

1. INTRODUCTION

Previous work has shown that the intensity of the equilibrated Hadley circulation in a zonally symmetric atmosphere will increase nonlinearly as the magnitude of an off-equatorial heat source is enhanced beyond a threshold value (Plumb and Hou 1992) or as the maximum of a meridional heating profile is moved off the equator (Lindzen and Hou 1988). These findings suggest that an insolation forcing which varies with a smooth seasonal cycle may cause comparatively abrupt transitions in the Hadley circulation as the thermal forcing oscillates between regimes in which linear and nonlinear atmospheric responses are expected. On the other hand, the circulation may not always be in equilibrium with the thermal forcing. Fang and Tung (1999) found that there was no abrupt change in the Hadley circulation in a dry, zonally symmetric model as the maximum of the thermal forcing was moved meridionally in an annual cycle.

In the first part of this paper we present results similar to those of Fang and Tung (1999) but using a different thermal forcing, showing that an abrupt change in the Hadley circulation is not found in a dry, zonally symmetric model as the magnitude of an off-equatorial heat source varies with a smooth annual cycle. The next section explores the response of a zonally symmetric model configured with representations of moist convection, long- and shortwave radiation, and a land surface poleward of the equator in one hemisphere. Abrupt transitions between solsticial circulations do occur in this model and are found to result primarily from a wind-evaporation feedback. Moisture-radiation feedbacks play a role in setting the timing of this transition and the intensity of the peak circulation.

2. MODEL DETAILS

The model is a zonally symmetric (two-dimensional) version of the MIT GCM (Marshall et al. 2004), similar to that used in Pauluis and Emanuel (2004). The model domain is a partial (zonally symmetric) sphere extending from 64 N to 64 S, with 1-degree meridional resolution on a staggered spherical polar grid. There are 40 pressure levels with 25 hPa resolution, from 1000 hPa to a rigid lid at 0 hPa, and no representation of orography. Viscosity is represented by the vertical mixing of momentum with a coefficient of 100 Pa^2s^{-1}. The planetary boundary layer is represented by homogenizing horizontal velocities within the lowest 200 hPa of the atmosphere over a timescale of 20 minutes. An eighth-order Shapiro filter is used to reduce small-scale horizontal noise in the temperature, specific humidity, and horizontal wind fields.

3. DRY MODEL RESULTS

In a dry version of the model, the circulation is forced by relaxation of temperature to a prescribed distribution T_{eq} similar to that used by Plumb and Hou (1992), representative of an off-equatorial thermal forcing centered at latitude φ_0:

$$T_{eq} = T_0 + \theta_m \frac{\pi}{2} sin(\pi \frac{p_0 - p}{p_0}) cos^2(\frac{\pi}{2} \frac{\phi - \phi_0}{\Delta\phi}) \quad (1)$$

Expression (1) specifies T_{eq} between $\varphi_0 - \Delta\varphi$ and $\varphi_0 - \Delta\varphi$; outside this range we specify $T_{eq} = T_0$. Here φ_0 = 16 ˚S, $\Delta\varphi$ = 20˚, T_0 = 200 K, and the amplitude of the thermal forcing varies with a seasonal cycle:

$$\theta_m = 20 cos(2\pi \frac{t}{365}) \quad (2)$$

where t is time in days, so that θ_m has a maximum amplitude of 20 K.

The diagnostic used to represent the large-scale circulation is the meridional flow integrated both vertically through the boundary layer (1000 – 800 hPa) and meridionally over all model latitudes, hereafter referred to as the PBL flow. This measure of the circulation proves to be more useful than the spatial maximum of the overturning streamfunction when applied to the moist model integrations discussed in the next section. The circulation exhibits no abrupt transitions over time. The PBL flow varies nearly linearly with the forcing, with a phase lag that depends on the thermal relaxation timescale (Fig. 1).

4. MOIST MODEL RESULTS

4.1 Model description

In a moist version of the model, the circulation is forced by radiative cooling together with surface fluxes of latent and sensible heat which are vertically redistributed by moist convection. Surface fluxes are represented by a bulk parameterization. Radiation is calculated by the longwave scheme of Morcrette (1991) and the shortwave scheme of Fouquart and Bonnel (1980). Moist convection is represented by the scheme of Emanuel and Zivkovic-Rothman (1999), with partial cloudiness predicted according to Bony and Emanuel (2001). The lower boundary is an ocean surface having uniform sea surface temperature (SST) of 300 K. This highly idealized SST distribution was chosen to

* Corresponding author address: William R. Boos, Dept. of Earth, Atmospheric, and Planetary Sciences, Massachusetts Institute of Technology, 77 Massachusetts Ave., Cambridge, MA 02139; e-mail: billboos@mit.edu.

resemble the off-equatorial thermal forcing used in the dry model. Comparison with runs integrated with an SST gradient exhibited dynamically similar seasonal transitions, so that the uniform SST distribution may also serve to isolate the relevant physics. A land surface was included poleward of 16 ˚S (a Southern Hemisphere monsoon configuration), with ocean at all other latitudes. The hydrology of the land surface is represented by a simple bucket model adapted from Delworth and Manabe (1988), in which the soil mosture is altered only by precipitation and evaporation, with the potential evaporation being reduced by a factor linearly proportional to the soil moisture. The land surface temperature is predicted by an energy balance for a single soil layer of heat capacity 4×10^5 J m^{-2}.

4.2 Wind-evaporation feedback

The phenomenon of abrupt onset of the summer circulation is clearly illustrated by a clear-sky integration (conducted without cloud-radiative interactions, but with radiatively interactive water vapor), which we call the control run. In this model, the transition from peak winter to peak summer circulations takes about 50 days, and the PBL flow has a strong projection onto a step function (Fig. 2). This transition occurs more slowly in an integration conducted with the surface wind speed in the bulk ocean surface enthalpy flux parameterization fixed at the time mean value from the control run.

It is possible that some of the abruptness of the seasonal transition is due to fact that the insolation forcing includes harmonics with periods shorter than 365 days. In order to more clearly compare the circulation response with the forcing, we alter the model insolation to obtain a uniform length of day at each latitude, so that the maximum insolation merely translates meridionally with an annual cycle without varying in intensity. An abrupt transition of the circulation still occurs in this configuration, as can be seen when the PBL flow is plotted against the latitude of maximum insolation (Fig. 3). Suppressing the wind-evaporation feedback for this uniform length-of-day configuration results in a more elliptical phase-space trajectory. Note that these trajectories progress clockwise for the moist model, in which the PBL flow lags the latitude of maximum insolation, and counterclockwise for the dry model, in which the PBL flow leads the equilibrium temperature amplitude.

The SST gradient necessary to produce a meridional gradient of ocean evaporation equivalent to that induced by the wind-evaporation feedback is calculated by differentiating the bulk surface flux formula for the ocean evaporation *E*:

$$\frac{dE}{dy} = C_k(q^*(T_o) - q)\frac{d|\mathbf{V}|}{dy} + C_k|\mathbf{V}|\left(\frac{dq^*}{dT_o}\frac{dT_o}{dy} - \delta q\right) \qquad (3)$$

Here C_k is a transfer coefficient, **V** the surface wind velocity, q the specific humidity of the lowest atmospheric layer, and q^* the saturation specific humidity at ocean temperature T_o. The second term on the right hand side is zero for the control model run; we calculate the SST gradient needed to obtain the same value of *dE/dy* if the first term is instead set to zero. Taking the mean summer distribution of **V** from the control model integration yields an SST gradient of 0.27 K per degree latitude, while using **V** from the time of abrupt transition yields an SST gradient of 0.73 K per degree latitude (both of these calculations assume 80% relative humidity of the surface air).

These two time-invariant poleward SST gradients were imposed between 8 ˚S and the coastline at 16 ˚S in two model runs integrated without the wind-evaporation feedback (default clear-sky insolation with variable length-of-day was employed). About 20 days after the transition to the summer state, the run with the lower SST gradient exhibited a comparatively weak circulation with little cross-equatorial flow when compared to the run with a higher SST gradient (Fig. 4). This summer circulation in the run with high SST gradient compares well with that in the control run (i.e. the run with fully interactive surface fluxes).

4.3 Moisture-radiation feedbacks

Radiative feedbacks involving clouds and water vapor were found to delay the onset of the summer circulation and to almost double the magnitude of the peak summer PBL flow. These results are not illustrated here, and are the subject of further investigation.

5. DISCUSSION AND CONCLUSIONS

Numerous authors have speculated that the nonlinear dependence of the equilibrium response to an off-equatorial thermal forcing may be involved in the rapid onset of certain monsoon circulations (see, e.g., Xie and Saiki 1999, as well as a brief note in Plumb and Hou 1992). The fact that dry, zonally symmetric models forced by a smooth, seasonally varying thermal forcings exhibit no rapid transition between solsticial circulations suggests that such rapid onsets involve feedbacks between the circulation and diabatic heat sources. We have identified a wind-evaporation feedback as one possible mechanism for generating an abrupt onset of the summer circulation. Although evolution of the meridional SST gradient may also play a role in the seasonal transitions of monsoon circulations, our estimate suggests that, in the range of observed SST gradients, the wind-evaporation feedback may have a comparable contribution to the generation of surface enthalpy flux gradients.

Finally, it should be noted that the results presented here were fairly insensitive to the use of interactive soil moisture. This is somewhat surprising, given the fact that the formation of a thick, dry boundary layer over land was found to be of import in the process of monsoon onset in other studies (e.g. Xie and Saiki 1999). Future work will explore this issue.

6. REFERENCES

Bony, S., and K. A. Emanuel, 2001: A parameterization of the cloudiness associated with cumulus convection; Evaluation using TOGA COARE data. *J.Atmos.Sci.,* **58**, 3158-3183.

Delworth, T., and S. Manabe, 1988: Influence of potential evaporation on the variabilities of simulated soil wetness and climate. *J.Clim.,* **1**, 523-547.

Emanuel, K. A., and M. Zivkovic-Rothman, 1999: Development and evaluation of a convection scheme for use in climate models. *J.Atmos.Sci.,* **56**, 1766-1782.

Fang, M., and K. K. Tung, 1999: Time-dependent nonlinear Hadley circulation. *J.Atmos.Sci.,* **56**, 1797-1807.

Fouquart, Y., and B. Bonnel, 1980: Computation of solar heating of the Earth's atmosphere: A new parameterization. *Beitr.Phys.Atmos.,* **53**, 35-62.

Lindzen, R. S., and A. Y. Hou, 1988: Hadley circulations for zonally averaged heating centered off the equator. *J.Atmos.Sci.,* **45**, 2416-2427.

Marshall, J., A. Adcroft, J-M Campin, and C. Hill, 2004: Atmosphere-ocean modeling exploiting fluid isomorphisms. *Mon.Wea.Rev.,* **132**, 2882-2894.

Morcrette, J. -J., 1991: Radiation and cloud radiative properties in the European Centre for Medium-Range Weather Forecasts forecasting system. *J.Geophys.Res.,* **96**, 9121-9132.

Pauluis, O., and K. Emanuel, 2004: Numerical Instability Resulting from Infrequent Calculation of Radiative Heating. *Mon.Wea.Rev.,* **132**, . 673-686.

Plumb, R. A., and A. Y. Hou, 1992: The response of a zonally symmetric atmosphere to subtropoical thermal forcing: threshold behavior. *J.Atmos.Sci.,* **49**, 1790-1799.

Xie, S.-P., and N. Saiki, 1999: Abrupt onset and slow seasonal evolution of summer monsoon in an idealized GCM simulation. *J.Meteor.Soc.Japan,* **77**, 949-968.

7. FIGURES

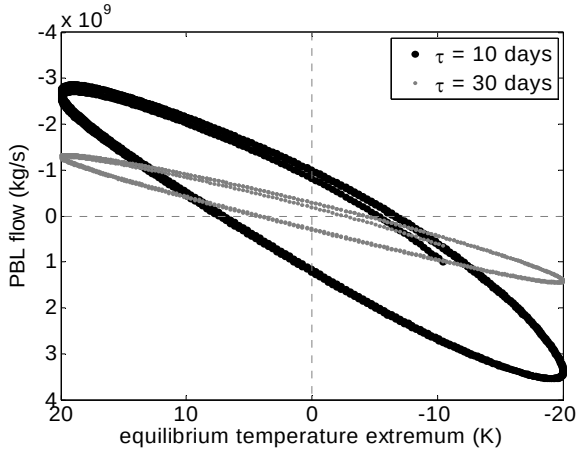

Fig. 1: Phase diagram of the integrated boundary layer flow (defined in the text) and the spatial extremum of the equilibrium temperature profile for the dry model. The thick, black curve corresponds to a thermal relaxation time of 10 days, and the thin gray curve to one of 30 days. Time progresses counterclockwise for both closed curves.

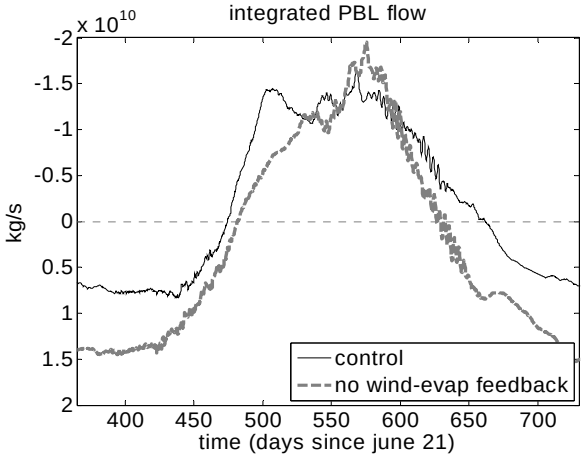

Fig. 2: Time series of the integrated boundary layer flow for the moist model with fully interactive surface fluxes (thin line) and a suppressed wind-evaporation feedback (thick dashed line). Time is the number of days since the (austral) winter solstice.

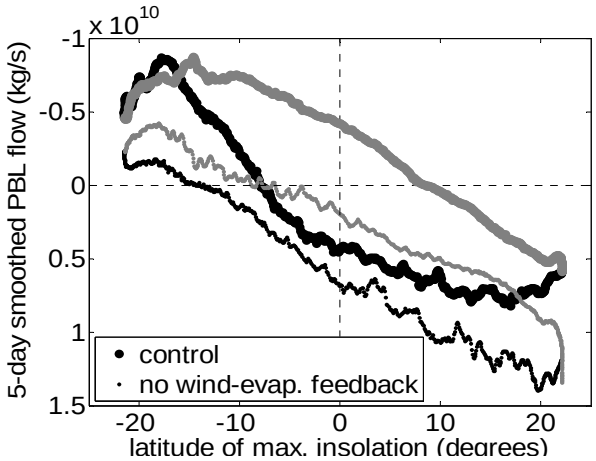

Fig. 3: Phase diagram of the integrated boundary layer flow and the latitude of maximum insolation for the moist model with clear-sky radiation and uniform length-of-day. The top closed curve is for the run with interactive surface fluxes, and the bottom for the run with the ocean wind-evaporation feedback suppressed (the black and grey colors denote the first and second halves of each year, respectively). Time progresses clockwise for both closed curves.

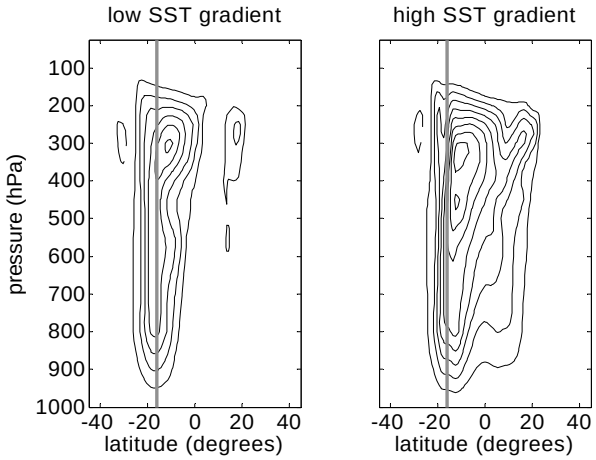

Fig. 4: The 5-day smoothed streamfunction for the moist model with the wind-evaporation feedback suppressed, and with an imposed SST gradient of 0.27 K per degree latitude (left) and 0.73 K per degree latitude (right). Both are for the model state 20 days after onset of the summer circulation. The thick vertical line denotes the latitude of the coastline (with land to the left). Solid contours denote clockwise rotation and negative contours counterclockwise rotation.